TECHNICAL UNIVERSITY OF CLUJ-NAPOCA

ACTA TECHNICA NAPOCENSIS

Series: Applied Mathematics, Mechanics, and Engineering
Vol. 66, Issue Special II, October, 2023

INFLUENCE OF FUSED FILAMENT FABRICATION RASTER PARAMETERS OVER THE TOP SURFACE TOPOGRAPHY

Vasile ERMOLAI, Alexandru SOVER, Gheorghe NAGÎȚ, Marius Andrei BOCA, Alexandru Ionuț IRIMIA

Abstract: *Fused Filament Fabrication builds parts layer-wise by depositing molten thermoplastic in the shape of filaments. Those are characterized by thickness and width. Together with the deposition speed, they determine the material flow. Depending on the extrusion system melting capacity and the considered materials, the flow can be limited to a certain degree, leading to under-extrusion. Slicing tools such as Cura allows filaments to overlap to compensate for under-extrusion and prevent voids formation. However, if the superposition is too high, the melt is squeezed out of the deposition path, affecting the surface quality. This study aimed to evaluate the influence of raster width, angle, overlap, and deposition speed over the top surface topography of samples printed of ABS, ASA, and PC. The results show that the rasters' width and overlap significantly influence top surface topography.*
Keywords: *Fused Filament Fabrication, Surface topography, Rasters parameters, Voids formation, Asperities formation.*

1. INTRODUCTION

Fused Filament Fabrication (FFF) is an extrusion-based process that uses thermoplastic materials to build parts additively [1-3]. The feedstock in the shape of a filament is fed into a heated zone, where it is liquified and forced through a nozzle and successively deposited in the shape of filaments (or lines) defined by width and thickness to form layers [2, 3].

As a structure, FFF printed parts are composed of constructive elements which describe the external and internal geometry. The external geometry consists of one or multiple shells (or walls) which are filled with rasters (or solid fill) at the level of the bottom and top layers. On the other hand, the internal geometry can be printed with a lower density than the external one to reduce material consumption and manufacturing time. This is known as infill and is characterized by pattern and density [4, 5].

Surface roughness is a technical requirement of any part and is used as an index to describe its quality. The FFF resulting parts have poor surface quality due to the staircase effect, geometry, and process parametrization. Starting with the geometry, the part's quality can be divided in side and top surfaces roughness [4, 6].

Side roughness defines the print quality of the outer shell and is influenced by the layer thickness. Several studies showed that surface finish can be improved by using lower layer thicknesses [4, 6-8].

Top surface roughness is influenced by multiple parameters such as shell width, raster width, angle, and air gap (overlap), and to a lower extent by process parameters such as printing speed and extrusion temperature [6, 8].

Nerveless the used polymer type (e.g., PLA, PA) and their filling agents (e.g., pigments) play and significant role in the filament process ability and the resulting part surface quality [4].

This study aimed to evaluate the influence of material raster width, angle, overlap, and deposition speed over the top surface topography of samples printed of ABS, ASA, and PC. The results show that the process parameters significantly influence top surface

topography through voids, asperities, and proper coalescence between the material lines.

2. METHODS

2.1 Design of experiment

The design of the experiment was realized based on a Taguchi L9 orthogonal matrix with four factors with three levels of variation, which describe the top surface of the parallelepipedal samples.

Using mesh modifiers (i.e., geometries that overlapped into the printing models to enable the local control of the process parameters [5, 9]), the parametrization described in Table 1 was applied only to the samples' top surface, which consists of two layers (see Fig. 1).

Table 1

Taguchi L9 (4^3) experimental matrix for printing the samples' top surface.

Run ord.	RW (mm)	RA (°)	RO (mm)	RPS (mm/s)
R1	0.4	0/90	0	20
R2	0.4	30/120	0.05	30
R3	0.4	45/135	0.1	40
R4	0.5	0/90	0	40
R5	0.5	30/120	0.05	20
R6	0.5	45/135	0.1	30
R7	0.6	0/90	0	30
R8	0.6	30/120	0.05	40
R9	0.6	45/135	0.1	20

RW – Raster width; RO – Raster overlap (air gap);
RA – Raster angle; RPS – Raster print speed.

RW controls the extrusion width of the top surface rasters. The lower level of the raster of 0.4 mm width will produce smaller air gaps between the deposition paths, and the upper one of 0.6 mm will increase voids size. Air gap formation can be further amplified if under-extrusion occurs during printing [9].

RA controls the solid fill's line orientation of the top surface. Raster angle is believed to influence air gap size between lines due to the print head movements [9].

RO describes the superposition between the extruded filaments. This parameter can influence the top surface quality. When the overlap is insufficient, voids occur between the rasters, and when if too high (negative air gap), the melt is forced out, creating scratches [9, 10].

RPS controls the rasters' deposition speed and depends on the polymer and extrusion system capacity to liquefy it to provide a constant material flow. If the extrusion system can't provide enough molten thermoplastic at the established deposition speed, under-extrusion can occur, which leads to air gap formation between rasters [9].

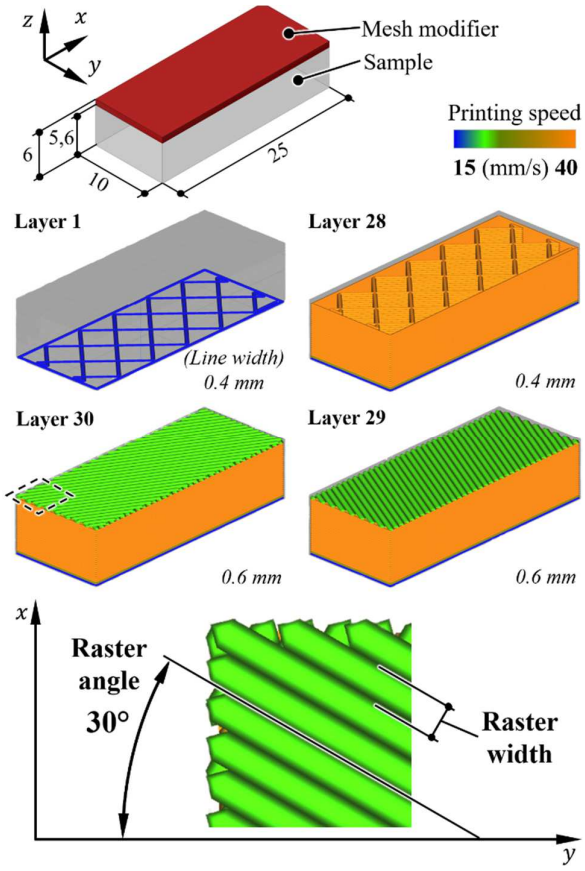

Fig.1. The effect of using mesh modifiers in the printing process of the top surface (R9 set-up of Table 1)

2.2 Samples' printing

The samples were printed using filaments from different manufacturers: a white color Ultrafuse ABS from BASF, a red ApolloX ASA from FormFutura, and a black PolyMax PC from Polymaker (see Fig. 2).

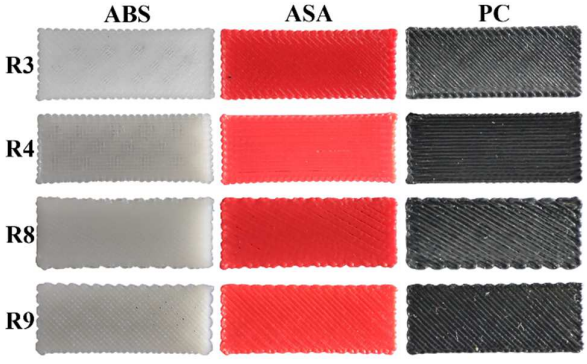

Fig.2. The resulting samples printed with R3, R4, R8, and R9 parametrizations of Table 1

The g-code manufacturing instructions were generated using Cura 4.13.1 slicing tool and the parametrization presented in Table 2 on an Ultimaker 3 printer. Only the top surfaces, which consist of two layers, were printed using the Taguchi L9 DOE (see Table 1). All samples were manufactured in a closed environment after the air temperature reached 40°C. A preview of the resulting samples is presented in Fig. 2.

Table 2

Main process parameters used for printing the samples [9].

No.	Parameter	Value
1	Nozzle diameter (mm)	0.4
2	Layer thickness (mm)	0.2
3	Extrusion width (mm)	0.4
4	Number of walls	1
5	Top/bottom layers	0
6	Infill pattern	Grid
7	Infill density (%)	25
8	Printing speed (mm/s)	35
9	First layer printing speed (mm/s)	15
10	Extrusion temperature (°C)	250/**255**/*265*
11	Bed temperature (°C)	100
12	Maximum fan speed (%)	3/**3**/*0*
13	Retraction distance (mm)	8/**7**/*7*
14	Retraction speed (mm/s)	30/**35**/*35*
15	Z seam position	Sharpest corner
16	Brim width (mm)	1.6
17	Enclosure	Yes

Values in bold are associated with the ASA filament;
Values in bold are associated with the PC filament.

3. RESULTS AND DISCUSSION

3.1. Top surface roughness

The optical analysis was carried out to characterize the top surface topography of the resulting samples. The study was performed using a Keyence Vhx 7000 digital microscope with a Vh-zst objective at 200x magnification.

The measurements were based on λ_c cut-off and λ_s shortwave profile filter (ISO 4288:1998). The cut-off is selected based on the surface valley spacing. The filaments' extrusion width gives the periodical profile for FFF printed parts. This way, for the samples printed with 0.4 mm RW, the used filters were λ_c=0.8 mm and λ_s=2.5 µm. For the other samples printed with 0.5 mm and 0.6 mm RW, the used filters were λ_c=2.5 mm and λ_s=8 µm. These filters were used to extract the Ra (i.e., the arithmetical mean deviation between valleys and peaks) and Rz (i.e., the maximum height of profile) roughness parameters by taking three measurements perpendicular to the rasters' angle. Because the mapped surfaces have an area of 1000x 1500 µm, the selected zones have been chosen to characterize both good and poor-quality regions (i.e., with voids and scratches).

The resulting average results and the standard deviations of the Ra, Rz roughness parameters are presented in Table 3. Even if the ABS, ASA, and PC were printed with the same parametrization (except for the extrusion temperature, cooling, and retraction, as shown in Table 2), the average results show a significant variation of the Ra and Rz.

Table 3

Means values and standard deviations of the Ra, Rz roughness parameters.

	ABS		ASA		PC	
	Ra (µm)	*Rz (µm)*	*Ra (µm)*	*Rz (µm)*	*Ra (µm)*	*Rz (µm)*
R1	3.7±1.2	14.8±6.8	3.1±1.3	17.4±7.4	3.3±0.4	17.3±3.9
R2	8.8±1.2	30.3±3.2	5.1±2.0	22.6±7.0	4.6±1.2	24.7±1.1
R3	8.6±3.6	30.9±2.7	2.1±0.6	10.0±2.2	3.6±1.2	20.7±2.9
R4	7.5±0.8	49.1±8.5	13.0±0.9	53.2±12.5	7.8±1.2	51.1±11.2
R5	5.1±2.3	33.6±10.8	7.7±1.9	32.5±8.5	6.4±1.4	44.1±7.6
R6	7.3±2.2	35.7±6.1	9.7±0.7	48.3±8.9	7.8±1.9	45.6±9.1
R7	10.8±2.9	66.2±13.1	10.9±1.6	52.0±3.5	13.3±2.2	70.7±8.7
R8	15.2±2.6	59.4±3.5	13.3±5.4	67.8±24.2	17.4±7.5	81.5±22.9
R9	11.8±5.0	62.3±15.6	12.0±1.6	52.5±12.5	12.6±2.3	75.9±9.2

, where R represents the run order.

By analyzing the bar charts presented in Fig. 3, it can be observed that the average Rz values are increasing proportionally with the increase of the raster width. Regardless of the used material, ABS, ASA, or PC, the resulting top surfaces showed comparable variation intervals among every nine parametrizations.

Samples printed with R1 to R3 set-ups resulted in an average Rz of 10.0-30.9 µm, the ones printed with R4 to R6 resulted in 32.5-53.2 µm Rz, and samples from R7-R9 presented Rz values of 52.0-81.5 µm. As the analyzed zones include good and low-quality surfaces, the recorded standard deviations (see Table 3) vary between ±1.1 and ± 24.2 µm.

For ABS samples based on the Rz values, the best result was obtained by the R1 resulting surface printed with 0.4 mm easter width with a 0°/90° raster angle with no overlap between the rasters at a speed of 20 mm/s. The resulting surface shows an Rz of 14.8±6.8 µm.

The same parametrization (R1) provided the best surface quality for the PC samples, having an average Rz of 17.0±4.4 µm. However, comparable results were obtained with the R2 (i.e., 24.7±1.1 µm) and R3 (i.e., 20.7±2 µm), printed with different raster orientations, overlap, and deposition speeds (see Table 1).

For ASA samples, the lowest Rz average values, of 10.0±2.2 µm, were obtained by using the R3 parametrization, in which the rasters of 0.4 mm width were printed with 45°/135° orientation and 0.1 mm overlap at 40 mm/s.

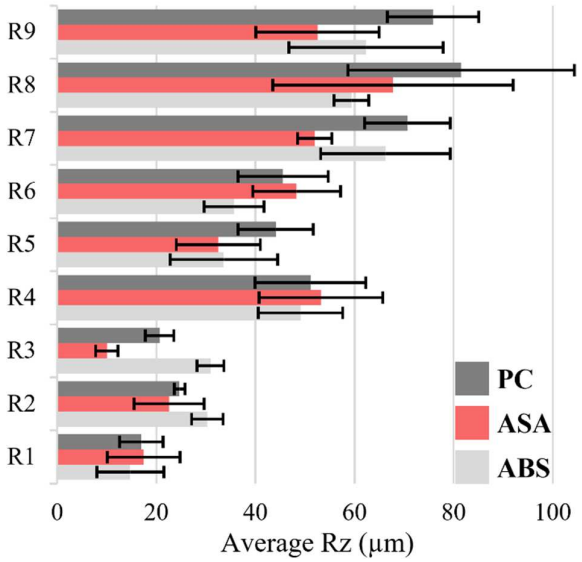

Fig.3. Mean values of the Rz roughness parameter

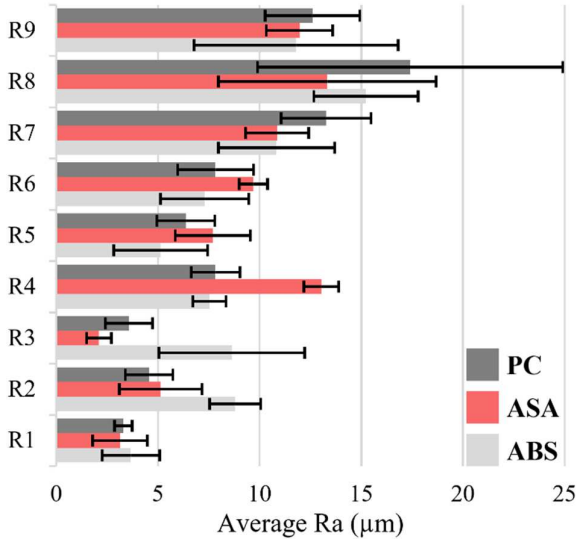

Fig.4. Mean values of the Ra roughness parameter

The bar plots of the Ra roughness parameter show the arithmetic mean of the all-profiles values (see Fig. 4). Considering the ISO 1302:2002 roughness grade numbers, the best resulting Ra values fitting in the N9 class, out of twelve, with maximum Ra of 6.3 µm, and belong to the R1 parametrization for ABS, R1 to R3 for ASA and PC (see Table 3).

Four resulting 3D surfaces were analyzed for each of the three materials to understand better the considered factors' effect on top surface topography. On the one hand, the R3, R4, and R8 resulting samples were selected because they were printed with the same speed of 40 mm/s (i.e., the upper level) and different levels of the other parameters. On the other hand, the R9 parametrization was considered because it was printed at 20 mm/s (i.e., the lower level) and presented different surface topographies for the three materials.

The top surfaces resulting from the R3 parametrizations are characterized by a raster width of 0.4 mm with 45°/135° orientation and 0.1 mm overlap. As presented in Fig. 5, the difference between surfaces' valleys and peaks is 43.5 µm for ABS, 46.4 µm for ASA, and 76.2 µm for PC. As observed, the 0.1 mm overlap between rasters has a different effect depending on the material.

The ABS-printed surfaces present multiple peaks (i.e., asperities) with a deviation of the periodical profile imposed by the raster width compared to the PC-printed surface. However, the same printing setup provided better surface quality when printing with ASA (see Fig. 5).

The R4 surfaces were printed with 0.5 mm raster width having an 0°/90° angle and 0.05 mm overlap. As shown in Fig. 6, regardless of the material, each resulting surface presents voids between the rasters, with comparable sizes of 78.0-89.7 µm. More than that, the same printing parameters can influence the shape of the extruded filaments differently due to extrusion inconsistencies. This way, the filaments present a certain degree of waviness on the sides. This effect can be attributed to the inconsistent melt flow during printing due to higher raster width and deposition speed or due to the low capacity of the extruder to melt the 2.85 mm filament.

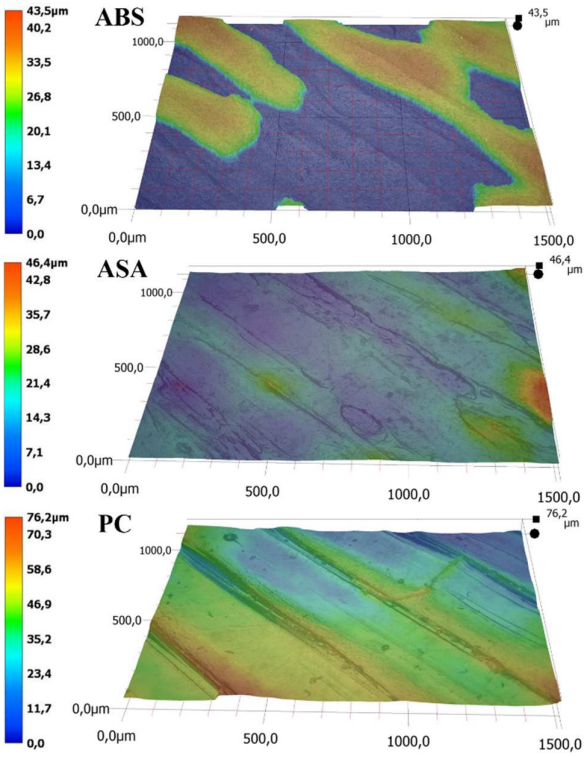

Fig.5. Surface topography of the R3 printed samples

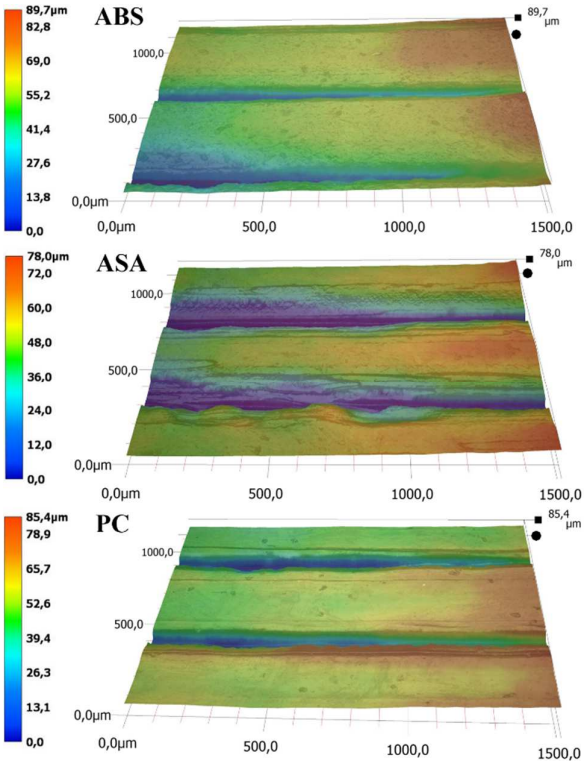

Fig.6. Surface topography of the R4 printed samples

The R8 samples were printed with 0.6 mm raster width, an orientation of 30°/120°, and without overlap between the filaments. As presented in Fig. 7, the resulting surfaces present higher voids between the rasters than those from the R4 parametrization. As previously observed, the topography of the resulting surfaces is different between materials. This way, for the R4 setup, the smallest voids were obtained by the ABS surface, followed by the PC and ASA. For the last one, the difference between the highest peak and valley is 207.1 µm. The identified valley (i.e., the blue color region) is the top surface of the substrate layer. This way, the resulting void has a depth approximatively equal to the chosen layer height of 0.2 mm (see Table 2). A similar pattern of voids was observed for surfaces printed with ABS but with smaller voids, up to 128.0 µm depth.

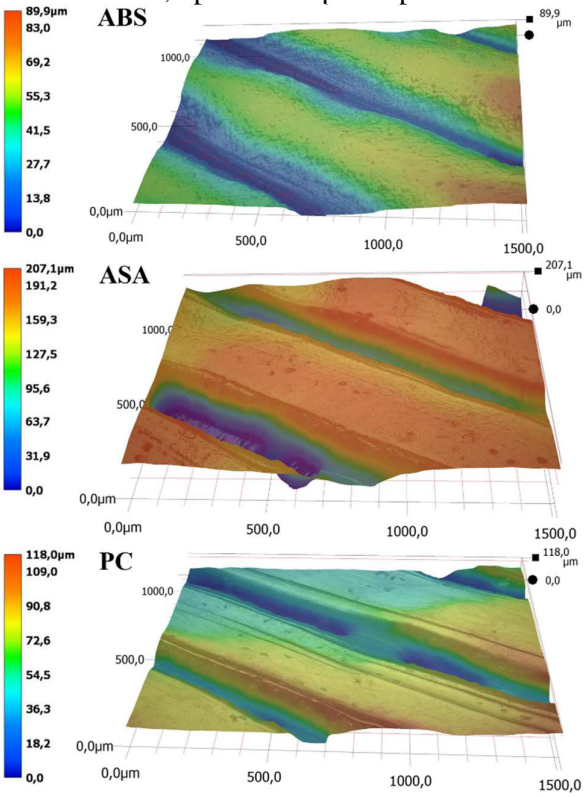

Fig.7. Surface topography of the R8 printed samples

Fig. 8 shows the resulting samples of the R9 top surface parametrization with 0.6 mm raster width with a 45°/135° orientation, having a superposition of 0.05 mm and printed at the speed of 20 mm/s. Even if the low deposition speed theoretically dives the extrusion system more time to melt the material, the resulting surfaces are characterized by voids between rasters. The highest depth of the voids was

obtained for the ABS (209.9 µm) material and followed by PC (148.4 µm) and ASA (81.9 µm). Correlated with the results obtained for the R8 parametrization surfaces, printed with 40 mm/s compared to 20 mm/s, it can be stated that the printing speed doesn't significantly influence the void formation between rasters. Similar studies showed that the deposition speed has a reduced influence over FFF printed surface quality [4, 11].

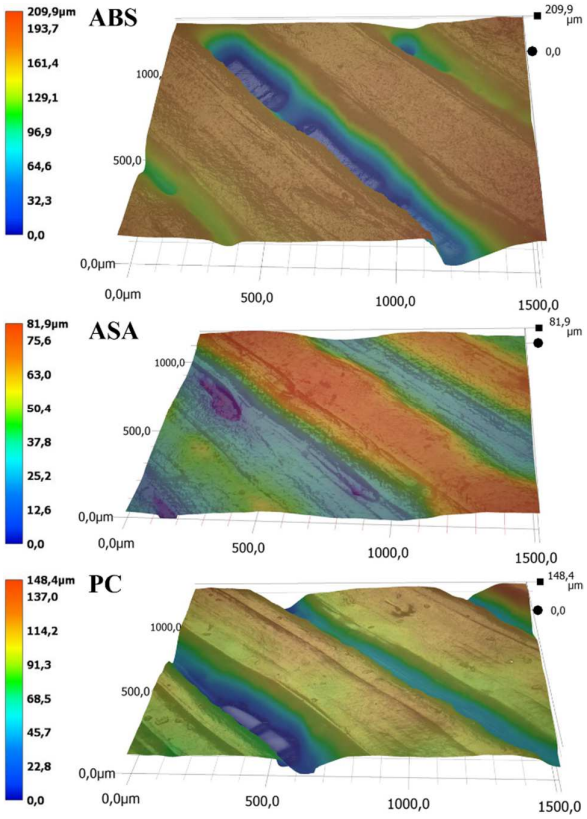

Fig.8. Surface topography of the R9 printed samples

3.2. Variables effects

The resulting Rz roughness parameter values were used as an output variable to analyze the Taguchi L9 experimental matrix. This way, the variables' main effects plots, and significance were determined using Minitab 21 statistical tool. As shown in Table 4, regardless of the used material, the variables have the same influence over the surface roughness. This way, the most significant factor for the surface roughness is the raster width, followed by the raster overlap, deposition speed, and angle.

By analyzing the delta values and the factorial plots (see Fig. 9), it can be observed that variable' levels have different influences over the surface roughness depending on the material. On the one hand, to reduce the top surface roughness, the raster width and printing speed variables should be set at the lower level. On the other hand, for raster overlap and angle, the optimal level should be selected depending on the considered material, ABS, ASA, or PC.

Table 4

Size of the main effects based on the average Rz values and the resulting ranks of the factors.

Material	Raster width (mm)	Raster angle (°)	Raster overlap (mm)	Print speed (mm/s)
	25.33	43.37	36.60	36.91
ABS	39.47	41.10	47.24	44.07
	62.64	42.98	43.60	46.47
Delta	37.31	2.27	10.64	9.96
Rank	**1**	**4**	**2**	**3**
	16.68	40.89	44.51	34.16
ASA	44.69	40.94	42.78	40.97
	57.43	36.97	31.51	43.68
Delta	40.76	3.98	13.00	9.52
Rank	**1**	**4**	**2**	**3**
	20.79	46.27	48.14	45.77
PC	46.93	50.11	50.57	46.98
	76.02	47.37	45.14	51.11
Delta	55.23	3.38	5.42	5.46
Rank	**1**	**4**	**2**	**3**

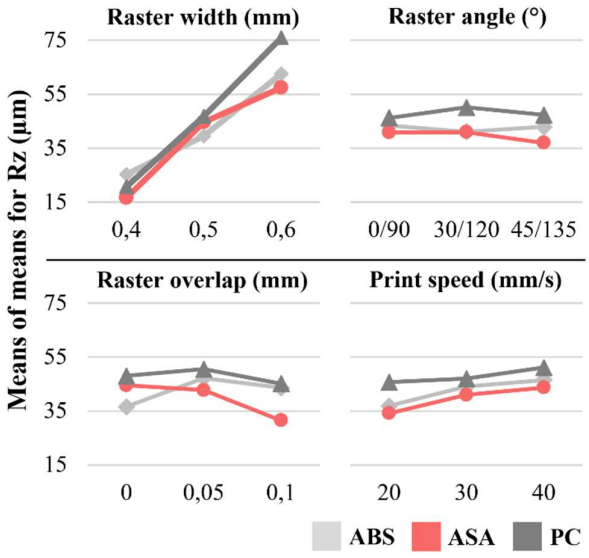

Fig.9. Main effect plots of the resulting Rz average values of Table 1 for ABS, ASA, and PC

The interaction plots in Fig. 10 provide additional information regarding the optimal level for the raster overlap, direction, and printing speed. As presented below, different

overlapping degrees and printing speeds are needed for each raster's direction to minimize the top surface roughness. For example, for the 0°/90° raster's orientation, the minimum surface roughness can be obtained by printing them with no overlap and at 20 mm/s. For the 30°/120° orientation comparable result can be obtained by printing the filaments with 0.05 mm overlap at 30 mm/s, as for the 45°/135° by printing the rasters at 40 mm/s with 0.05 mm overlap.

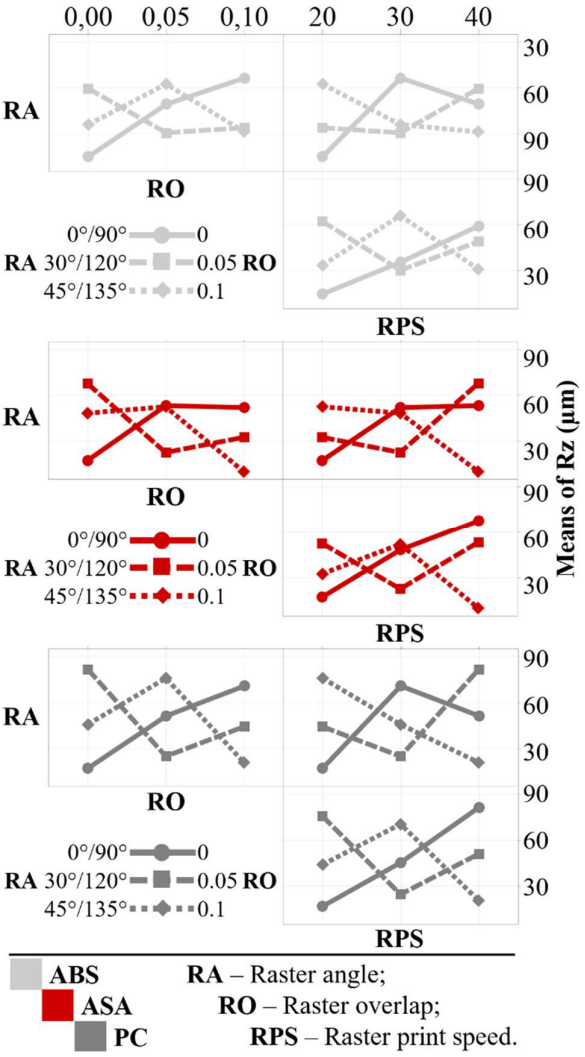

Fig.10. Interaction plots of the resulting Rz average values of Table 1 for ABS, ASA, and PC

4. CONCLUSIONS

In FFF 3D printing, the top surfaces of a part are created in layers by multiple passes of the printing head, which extrudes filaments, a defined cross-section, orientation, and overlapping. This way, each top surface is characterized by a periodical profile given by the extruded filament width and overlapping, influencing the resulting surface roughness. To this is added the deposition speed, which must consider the extrusion system melt capacity.

The top surfaces analyses of the ABS, ASA, and PC samples showed that the same process parameterization in terms of raster width, angle, overlap, and deposition speed provided different roughness values of the surfaces.

From the main effects plots, the raster width strongly influences the top surface roughness, followed by the raster overlap, sprinting speed, and angle.

Overall, the top surface quality can be improved by reducing the raster width and deposition speed for the considered ABS, ASA, and PC filaments. However, the optimal level should be selected for the other two variables depending on the material and their interactions with the other variables.

Further studies are needed to characterize how other combinations of the considered variables levels can further improve the top surface quality and if high-flow extrusion systems can reduce the formation of the voids between filaments.

5. REFERENCES

[1] Gibson, I., Rosen, D., Stucker, B., Khorasani, M. *Material extrusion*, In Additive Manufacturing Technologies, Springer Nature, Switzerland, ISBN 978-3-030-56127-7, 171-201, 2021.

[2] Singh, S., Singh, G., Prakash, C., Ramakrishna, S., *Current status and future directions of fused filament fabrication*. J. Manuf. Process. 55, 288-306, 2020. https://doi.org/10.1016/j.jmapro.2020.04.049

[3] Saleh Alghamdi, S., John, S., Roy Choudhury, N., Dutta, N. K., *Additive manufacturing of polymer materials: Progress, promise and challenges*. Polymers, 13(5), 753, 2021. https://doi.org/10.3390/polym13050753

[4] Dey, A., Yodo, N., *A systematic survey of FDM process parameter optimization and their influence on part characteristics*. J.

Manuf. Mater. Process. 3(3), 64, 2019. https://doi.org/10.3390/jmmp3030064

[5] Stavarache, R.C., Ermolai, V., Ripanu, M.I., Andruşcă, L., Mareş, M., Dodun, O., *Infill pattern optimization of fused filament fabrication samples for enhanced mechanical properties*. Sci. Bull. Ser. C Fascicle Mech. Tribol. Mach. Manuf. Technol., 2021, 35, 80-85.

[6] Lokesh, N., Reddy, J. S., Praveen, B.A., Veeresh, Y.K., Sreehari Acharya, B., Kapse, J.E., Prasad, M., *Evaluation and Optimization of Process Parameter for Surface Roughness of 3D-Printed PETG Specimens Using Taguchi Method at Constant Printing Temperature*. In Recent Adv. Mech. Eng.: Select Proc. of ICRAMERD 2021. Springer Nature, Singapore, 201-212. https://doi.org/10.1007/978-981-16-9057-0_22

[7] Altan, M., Eryildiz, M., Gumus, B., Kahraman, Y., *Effects of process parameters on the quality of PLA products fabricated by fused deposition modeling (FDM): surface roughness and tensile strength*. Materials Testing, 60(5), 471-477, 2018. https://doi.org/10.3139/120.111178

[8] Mushtaq, R. T., Iqbal, A., Wang, Y., Cheok, Q., Abbas, S., *Parametric Effects of Fused Filament Fabrication Approach on Surface Roughness of Acrylonitrile Butadiene Styrene and Nylon-6 Polymer*. Materials, 15(15), 5206, 2022. https://doi.org/10.3390/ma15155206

[9] Ermolai, V., Sover, A., Nagîţ, G. *Influence of bond interface over the lap-shear performance of 3D printed multi-material samples.* In MATEC Web of Conf. (Vol. 368). EDP Sciences, 2022. https://doi.org/10.1051/matecconf/202236801005

[10] Tao, Y., Kong, F., Li, Z., Zhang, J., Zhao, X., Yin, Q., Li, P., *A review on voids of 3D printed parts by fused filament fabrication*. J. Mater. Res. Technol. 15, 4860-4879, 2021. https://doi.org/10.1016/j.jmrt.2021.10.108

[11] Beșliu-Băncescu, I., Tamașag, I., Slătineanu, L., *Influence of 3D Printing Conditions on Some Physical–Mechanical and Technological Properties of PCL Wood-Based Polymer Parts Manufactured by FDM*. Polymers, 15(10), 2305, 2023. https://doi.org/10.3390/polym15102305

Influența parametrilor de extrudare asupra topografiei suprafețelor superioare pentru procedeul de fabricație cu filament fuzibil

Fabricația cu filament fuzionat permite construcția pieselor într-un mod stratificat prin depunerea de material termoplastic topit sub formă de cordoane, iar fluxul de material necesar extrudării este definit prin lățimea, grosimea și viteza de depunere a acestora. În funcție de capacitatea de topire a sistemului de extrudare și de materialele utilizate, fluxul poate fi afectat, ducând la subextrudare. Programe de secționare precum Cura, permit suprapunerea filamentelor pentru a limita subextrudarea și formarea de goluri între acestea. Cu toate acestea, dacă suprapunerea este prea mare, materialul topit este forțat în afara traseului de depunere, formând asperități la nivelul superfeței superioare. Studiul de față a urmărit evaluarea modului în care lățimea, orientarea, suprapunerea și viteza de depunere a cordoanelor influențează topografia suprafețelor superioare pentru piese printate din ABS, ASA și PC. Rezultatele arată că lățimea și suprapunerea cordoanelor de material influențează în mod semnificativ starea suprafețelor.

Vasile ERMOLAI[1], PhD student, vasile.ermolai@student.tuiasi.ro, vasile.ermolai@hs-ansbach.de
[1]Department of Machine Manufacturing Technology, "Gheorghe Asachi" Technical University of Iași, Romania
Alexandru SOVER[2], PhD Eng., Professor, a.sover@hs-ansbach.de
[2]Ansbach University of Applied Science, Faculty of Technology, Residenzstraße 8, Ansbach, 91522, Germany.
Gheorghe NAGÎȚ[1], PhD Eng., Professor, nagit@tcm.tuiasi.ro
Marius Andrei BOCA[1,2], PhD student, marius-andrei.boca@student.tuiasi.ro, marius-andrei.boca@student.tuiasi.ro
Alexandru Ionuț IRIMIA[1], PhD student, alexandru-ionut.irimia@student.tuiasi.ro